



Statistical Analysis of Nighttime TEC Depletions and GPS Loss of Lock in the Crest of Anomaly Region

Shivalika Sarkar* and A. K. Gwal**

*Regional Institute of Education, Shyamla Hills Bhopal, (Madhya Pradesh), INDIA

**Department of Physics, Barkatullah University Bhopal, (Madhya Pradesh), INDIA

(Corresponding author: Shivalika Sarkar)

(Received 02 October, 2017 accepted 12 November, 2017)

(Published by Research Trend, Website: www.researchtrend.net)

ABSTRACT: Depletions in nighttime total electron content (TEC) near the crest of equatorial ionization anomaly (EIA), Bhopal (Geog. 23.2° N, 77.4° E, and MLAT 14.2° N) has been statistically studied for the solar minimum period 2005-06. TEC data is recorded by dual frequency GPS receiver which was installed at Space Science Laboratory, Bhopal. Observations suggest the presence of large depletions in TEC which are always accompanied with fast increase in the scintillation index. Rate of change of TEC index (ROTI) has been used as an irregularity index. Losses of lock occur during the encounter of the irregularity. It is observed that nighttime depletions in TEC are more frequent in winter, less during equinox and least in summer months. These irregularities can cause significant errors in GPS positioning.

Keywords: Total electron content, nighttime depletion, EIA, ROTI.

I. INTRODUCTION

Ionosphere is highly dynamic medium characterized by irregularities in electron density and it departs from its usual and quiet state due to disturbances. Ionospheric variability includes irregularities in which the electron density differs significantly from the ambient plasma. These irregularities can cause diffraction effects, on the signal passing through them, enhancements or depletions in the electron densities, loss of lock of the satellite link with the receiver etc. The region between $\pm 20^\circ$ geomagnetic latitude and extending from 60-200 kms in altitude is known as equatorial ionosphere. The electrons move as far as the geomagnetic latitude of 10° to 20° causing high concentration there. The strongest effects are observed at approximately $\pm 10^\circ$ magnetic latitude [1]. In the equatorial zone the ionospheric irregularities are generated by gradient drift and developed by Rayleigh- Taylor(R-T) instability mechanisms over the magnetic equator in the post sunset hours [2]. These irregularities which occur in the form of plasma depletions, are also known as bubbles and have scale sizes ranging over several decades of magnitude extending from a few millimeters to hundreds of kilometers. These irregularities are elongated along the magnetic field line with axial ratios of the order of 5 to 10. The depletions that originate over the magnetic equator in the post sunset hours extend in both horizontal and vertical directions.

Plasma depletions are irregularities of the largest scale sizes that are associated with the Equatorial Spread F (ESF), wherein the plasma density may be lowered by up to three orders of magnitude compared to the background plasma density [3]. The pre-reversal enhancement holds the key to the formation of irregularities. This causes a rapid uplifting of the F-region, and steepens the bottomside gradient leading to Rayleigh-Taylor instability. Soon after sunset, vertical plasma drift gradients form in the bottom side of the F-layer. The upward density gradient is opposite in direction to the gravitational force. This configuration is R-T unstable and allows plasma density irregularities to form. These irregularities can grow to become large ionospheric depletions often called equatorial plasma bubbles. The bubbles are upwelled by electrodynamic EXB drift over the magnetic equator and map down to off-equatorial locations along magnetic field lines in the form of "bananas". The characteristics of these depletions, that has been obtained mainly with the Jicamarca radar [4] and substantiated by the scintillation based instruments and Altair radar observations [5], are very well documented. These depletions are field aligned and involve the uplift of the entire flux tube. Signal fluctuations due to the F-region plasma density irregularities have been reported at a wide range of frequencies [6], even as high as 7 GHz [7].

The effects of ionization depletions on the Faraday rotation of geostationary satellites have been used along the amplitude scintillation to study the characteristics namely, the amplitude and east-west extent of the equatorial bubbles [8]. Examples of TEC depletions and associated irregularities in Faraday rotation angle (representative of the TEC of the ionosphere) on a VHF beacon at 136 MHz from a geostationary satellite recorded at equatorial and low-latitude station were reported by [9]. The bubbles were found to have steep walls on the leading and trailing edges evident from the large time rate of change of the Faraday rotation angle. Effects of scintillation on GPS-based navigation and communication systems have been extensively studied by many authors [10-14]. Scintillation of GPS satellite L1 signal has been used to study the latitudinal extent of the irregularity belt [13]. Theoretical and observational investigations indicate that these depletions are generated on the bottom side of the nighttime equatorial F-region and rise to higher altitude due to the non-linear evolution of the generalized Rayleigh-Taylor (R-T) and EXB plasma instabilities [2]. These depletions are field aligned and involve the uplift of the entire flux tube. Characteristics of VHF radio wave scintillations over a solar cycle (1983-1993) based on FLEET SAT data was found by [15] and they also found that the nighttime scintillation occurrence is inhibited during disturbed periods in the solar maximum epoch, whereas scintillation occurrence is enhanced during solar minimum period. Strong L-band scintillations require the presence of short (~20cm) coherence scale length in the UHF scintillation pattern obtained in the plane of the receiver [16]. This condition is satisfied near the Equatorial Ionization Anomaly (EIA) crest region and not near the dip equator. They suggested that irregularity power spectrum steepens towards the end of the decay phase of L-band scintillation and the residual large scale irregularities can focus the UHF signals in the plane of the receiver rendering the S4 indices greater than one. Using scintillation data at L-band frequency (1.575 GHz) obtained from 18 GPS receivers obtained at different locations in India under the GAGAN(GPS-Aided Augmented Navigation) project, spatial, temporal and intensity (S4 indices) characteristics of trans-ionospheric scintillation during low sun-spot activity period were investigated by [17]. Occurrence of scintillation was found to maximize at pre midnight hours during equinoctial months. Post midnight scintillations were sparse. Scintillation events were also observed to be almost insignificant during summer and winter months. Intensity of scintillation was stronger around the belt of EIA and these scintillation events were mostly associated with TEC depletions. During the period of observations they found loss of lock events

when intense scintillation activity ($S_4 > 0.45 \sim 10\text{dB}$) was present in the Indian EIA region. The duration, magnitude and positional accuracy of these scintillation events were found to range from 5 to 25 min, 5 to 15 TEC units and 1 to 3m respectively. TEC and scintillations bite-outs in TEC were observed in conjunction with the amplitude scintillation by [18]. Occurrence of TEC fluctuations and its potential effect on GPS was studied by [19]. In another study by [20] total electron content (TEC) fluctuations and their regional differences over China were analyzed by utilizing the rate of the TEC index (ROTI) based on GPS data from 21 reference stations across China during a solar cycle. According to [20], strong ionospheric TEC fluctuations were usually observed at lower latitudes in southern China, where the occurrence of TEC fluctuations demonstrated typical nighttime- and season-dependent (equinox months) features. The monthly and seasonal variability of TEC and amplitude scintillation index (S_4) over two Indian polar stations Maitri (Antarctic) and NyAlesund (Arctic), during the low solar activity period 2008 was studied by [21]. In the present era of satellite based communication and navigation, the presence of ionospheric irregularities may result in loss of lock of the GPS signals and in most cases may cause degradation of signal amplitudes. Therefore it is very important to understand the various characteristics of ionospheric irregularities in detail. In this paper we have presented the first observations of nighttime TEC depletions (Plasma bubbles) at Bhopal (23.2°N , 77.4°E), a station near the northern crest of EIA using GPS derived TEC, for the period of low solar activity from January 2005 to December 2006. The statistics of nighttime TEC depletions have also been presented.

II. DATA AND METHODOLOGY

Scintillation and TEC data recorded during 2005 to 2006 by a GPS Ionospheric Scintillation and TEC monitor system (GISTM); GSV4004A installed at Department of Physics, Barkatullah University, Bhopal (23.2°N , 77.4°E , Geomagnetic 14.2°N) has been used to study the occurrence of nighttime depletions and associated scintillations. Study of loss of lock of GPS signals has also been studied. Amplitude scintillation is measured by S4 index defined as the standard deviation of the received signal power normalized to average signal power as follows:

$$S_{4T} = \sqrt{\frac{\langle P^2 \rangle - \langle P \rangle^2}{\langle P \rangle^2}}$$

Where $\langle \rangle$ represents the average values over a 60-second interval. The total S4 (S_{4t}) defined in above equation has significant amount of ambient noise associated with it, which has to be removed before further analysis. This is achieved by estimating the average signal-to-noise density (S/N) over a 60-second interval. This estimate is then used to determine the expected S4 due to ambient noise (also known as S4 correction) as follows:

$$S_{4N_0} = \sqrt{\frac{100}{S/N_0} \left[1 + \frac{500}{19S/N_0} \right]}$$

Replacing the S/N_0 with the 60-second estimates, S/N_0 , gives the S4 due to noise. The corrected S4 (ambient noise free) is then calculated in post processing as follows:

$$(S_4) = \sqrt{(S_4)_{tot}^2 - (S_4)_{cor}^2}$$

where $(S_4)_{tot}$ and $(S_4)_{cor}$ are total and corrected S4 respectively. In the present study, we have considered only those case which have amplitude scintillation $S_4 > 0.25$ index. The line of slant TEC is the measure of the number of electrons in a vertical column having a one square meter cross section, extending all the way from the GPS satellite to receiver and is reported in TEC Units ($1 \text{ TECU} = 1 \times 10^{16} \text{ Electrons/m}^2$). The total number of free electrons is proportional to the ionospheric difference delay of L1 and L2 signal and STEC is calculated as:

$$\text{STEC} = [9.483 * (\text{PRL2} - \text{PRL1}) + \text{TEC}_{RX} + \text{TEC}_{CAL}] \text{TECU}$$

Where PRL2 is the L2 pseudo-range and PRL1 is the L1 pseudo-range in meters, TEC_{RX} is the nominal L1/L2 receiver delay (converted to TECU) hard-coded as a data base parameter, and TEC_{CAL} represents the bias error correction and is different satellite-receiver pairs.

To study the ionospheric irregularity the rate of the TEC index (ROTI, in TECU/min) was proposed by [22]. The index ROTI is defined as the standard deviation of ROT over a 5 min time interval, as shown in Equation

$$\text{ROTI} = \frac{\Delta \text{STEC}}{\Delta t}$$

$$\text{ROTI} = \sqrt{\langle \text{ROT}^2 \rangle - \langle \text{ROT} \rangle^2}$$

where STEC represents the TEC along the ray path from the satellite to the receiver (in TECU) and Δt (in seconds) denotes the sampling interval.

The elevation angle of the GPS satellite plays an important role in determination of the ionospheric pierce point (IPP) altitude. The IPP is the parameter that represents the assumed altitude of the centroid of mass of the ionosphere which is mostly used in the calculation of irregularity drifts [23]. For the purpose of TEC analysis, ionospheric data is considered above 30° elevation of satellites in order to eliminate the errors due to multipath.

III. OBSERVATIONS AND RESULTS

TEC depletions and associated scintillations including loss of lock events during the low solar activity period 2005-2006 are presented and discussed in this paper. During this period we observed TEC depletions in 59 events in individual PRNs. Only those cases are considered in which maximum TEC depletion was larger than 1 TECU relative to the background TEC. Selected results for different satellites passes, designated by a Pseudorandom number (PRN) on different dates, are shown in the following figures. Each of the figures has four panels; the horizontal X axis of each panel corresponds to the Universal Time (UT). Top panel of each figure shows the Geomagnetic Latitude and Geographic Longitude of the ionospheric Pierce Point (IPP) computed from the elevation and azimuthal angles of the satellites at each instance of its pass, as seen from Bhopal. For IPP computation, a thin ionospheric shell at an altitude of 350 Km was assumed. The second panel gives the variations of the satellite elevation angle. The third panel gives the rate of TEC index (ROTI) for 5 minutes interval and the fourth panel (bottom panel) shows the TEC (left panel) and amplitude scintillation S4 (right panel). The sky plot of the satellite gives the information about the path of the different satellites (PRNs) in the sky with respect to the receiver. Therefore in order to clearly see the direction of the motion of the satellites, we draw sky plots of only those PRNs which have loss of lock during the period of the plasma bubbles. In these figures the big red dot at the centre shows the receiver position which is the overhead position for the satellite (zenith). Six concentric circles show the elevation angles (75° , 60° , 45° , 30° , 15° and 0°) of satellite with respect to the receiver towards outside the centre respectively. We have observed sudden depletions in TEC of short duration (less than an hour or around half an hour). Sudden decrease in TEC cannot be account for change in elevation angle or latitudinal variation and is the manifestation of the plasma bubbles [24-26]. A TEC depletion associated with equatorial plasma bubble has been defined by [24]. Accordingly, the TEC depletion consists of a sudden reduction in TEC followed by a recovery to a level near the TEC value preceding the depletion.

Processes such as the night time decay of the F-layer and the density redistribution caused by the Fountain effect also tend to decrease the TEC values [26]. But these processes result in shallow TEC slopes and an absence of the recovery segment. TEC depletions are a manifestation of the equatorial plasma depletion [27].

A. Depletions in TEC

Fig. 1 presents the results for satellite PRN 21 on 7 January 2005. The top panel of the figure shows the GMLAT and Geographic longitude of the IPP for this satellite pass. In this panel the blue line shows the GMLAT and green line shows the longitude of the IPP. It can be seen from the top panel that the GMLAT of the IPP varies from about 19° N to 8° N, its longitude varies from 74° E to 82° E, for the entire pass of the satellite. The second panel shows the satellite elevation angle with UT, and its highest elevation angle is 60° with respect to the site of observation. The ROTI value shows the strength of each irregularity shown in the third panel. This is confirmed by the sudden TEC depletion and increase in the S4 value. Hence ROTI can alone be used as the irregularity index. The variation of the TEC and S4 index is shown in the bottom panel of the Fig. 1. It can be seen from Fig. 1 that the TEC values decrease gradually with increasing satellite elevation angle; reaching a broad minima at the highest elevation angle

attained by the satellite prior to 15:30 UT. Thereafter, the TEC increases as the elevation angle decreases. This variation can be explained in terms of the variation in the slant length. There is a sudden reduction in TEC around 15:50 UT and it has been identified as a plasma depletion, wherein the TEC decreased by about 6 TEC units. The S4 index is less than 0.2 prior to the appearance of the depletion in TEC and it suddenly reaches to a value of about 0.4, coinciding with the occurrence of the depletion. From Fig. 1 it is clear that the GMLAT of IPP varies from about 15° N to 12° N. Thus, the depletion is far away from the magnetic equator. Its longitude is however, nearly constant around 78° E. The TEC value recovers after the dip and then increases thereafter.

One more case of depletion is observed on 17 February 2005 for PRN 15 shown in Fig. 2. In this case loss of lock is also observed during the time of depletion at 16:00 UT. The top panel of the diagram is a plot of the GMLAT and geographic longitude of the IPP for the satellite pass. The range of MLAT and longitude of the IPP is quite wide, about 19° N to 8° N; its longitude varies from 76° E to 79° E. The satellite elevation angle is observable about 45° above the horizon, and its highest elevation is about 85° with respect to the site of observation.

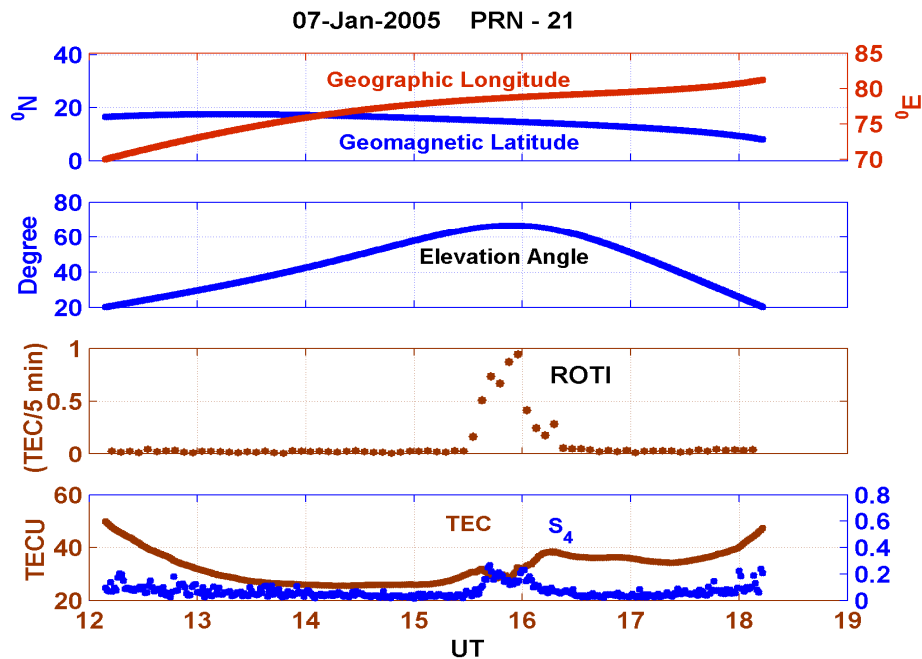


Fig. 1. Observations of depletion in TEC on 7 January 2005 for PRN-21. Top panel shows the ML at. and G. Long. of the ionospheric Pierce Point (IPP), second panel gives the satellite elevation angle. The third panel gives the rate of TEC index (ROTI) for 5 minutes interval and the fourth panel (bottom panel) shows the TEC (Left panel) and amplitude scintillation S4 (Right panel).

The variations in TEC are shown in the bottom panel of the Fig. 2. For the observed depletion, the MLAT of the IPP varies from about 18°N to 10°N. Thus the depletion is far away from the magnetic equator. The TEC value recovers after the dip and increases thereafter. A sudden drop in TEC reaching upto zero value, at the eastern end of the depletion, is a case of the cycle slip. In Fig. 3 (left panel) the lock time of PRN 15 is shown and it is clear that losses of lock occur during the encounter of the irregularity and the signal strength degrades during the

passes of the irregularity. It implies a sudden loss of phase lock of the signal due to increased scintillation activity (S_4 is about 0.6). The direction of motion of PRN 15 is north-south as clearly seen in Fig. 3 (Right panel). Normally, north-south satellite trajectories show scintillations over a long period with transition from intense scintillation to no scintillations or vice versa corresponding to crossing over the northern edge of the irregularity cloud.

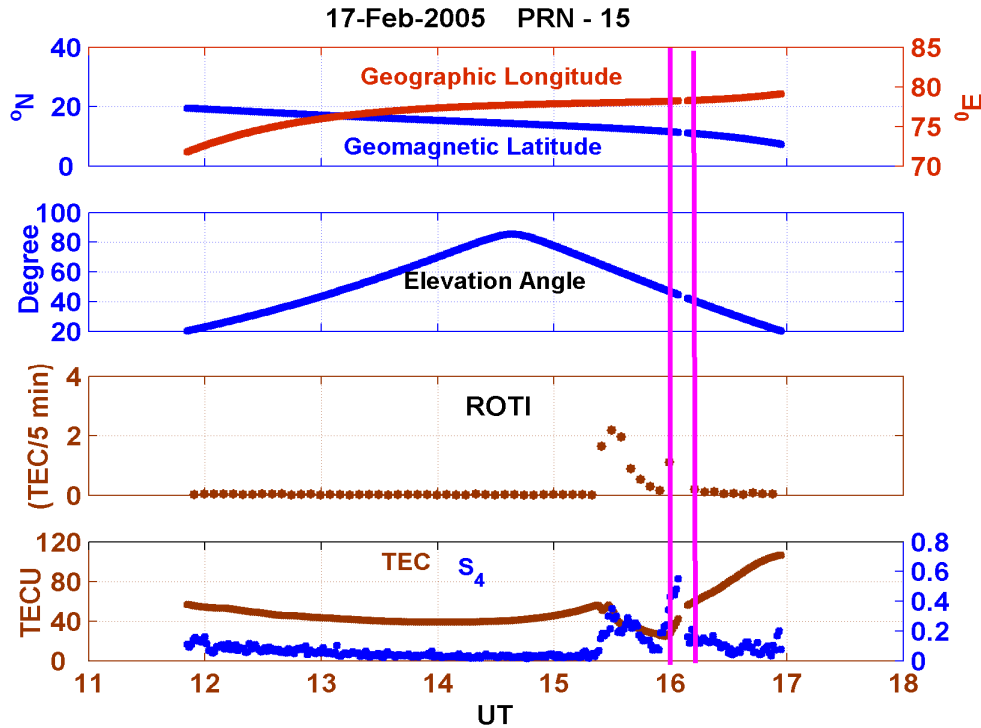


Fig. 2. Observations of depletion in TEC on 17 February 2005 for PRN-15. Same as Fig.1.

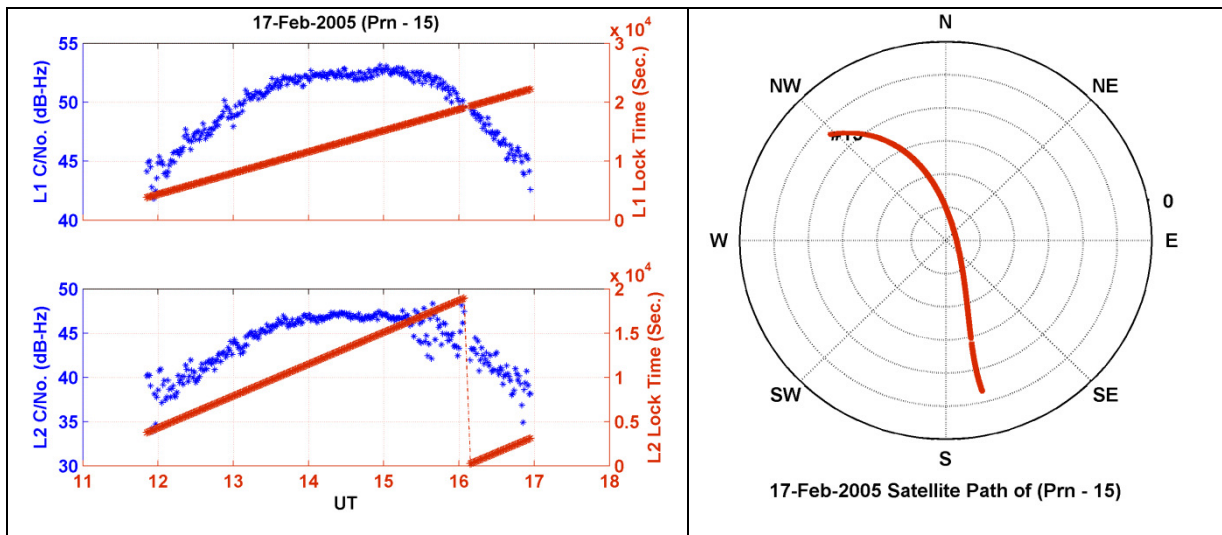


Fig. 3. Loss of lock of L1 and L2 signals and L1 and L2 carrier to noise ratio (Left panel) and Sky plot (Right panel) of PRN-15 for 17 February 2005.

Multiple depletions in TEC were observed on 13 October 2005 for PRN 5 is shown in Fig. 4. In this case the highest elevation attained by the satellite is about 65°. The IPP geographic longitude between the times of appearance of the two sets of depletions remains nearly constant and is about 76°E shown in the top panel of Fig. 4. This implies that these depletions are nearly field aligned and are occurring at well separated distances along the field lines. It can be seen in the third panel of the figure that ROTI shows significant variations during the time of depletion. Between the two sets of depletion

the variation in TEC is smooth and the scintillation index is at the noise level. The first region of depletion is occurring between 15:55 and 16:20 UT and the second region is between 17:00 and 17:15 UT. The latitudinal extent of IPP for the first region is from 14°N to 10°N and for second region it is 10°N to 8°N. The S4 index in these regions is very well correlated with the occurrence of depletion in TEC. The most important striking feature of the scintillation index is the complete absence of scintillations between the two sets of depletions. This is also the region where the TEC variation is smooth.

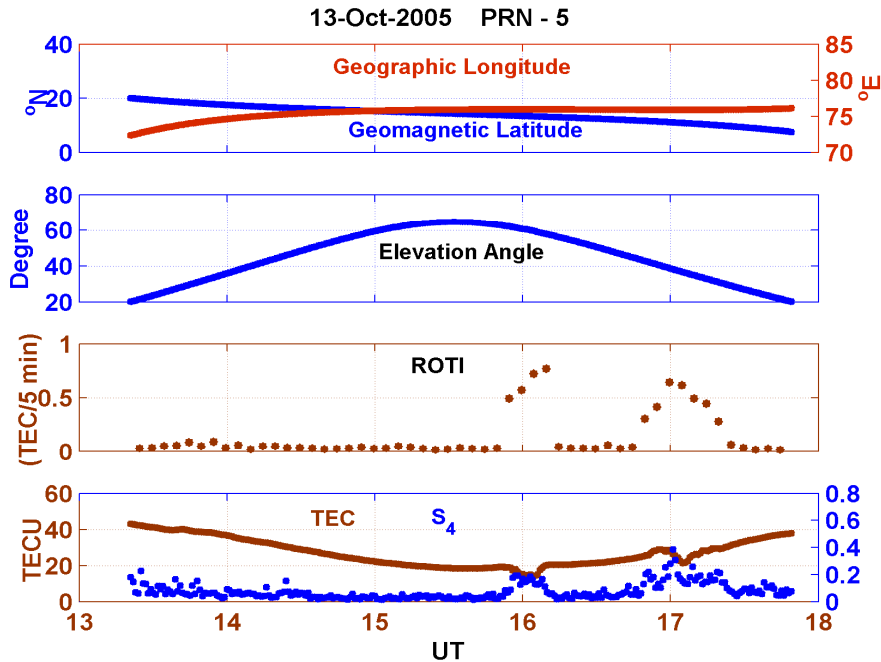


Fig. 4. Observations of depletion in TEC on 13 October 2005 for PRN-5. Same as Fig. 1.

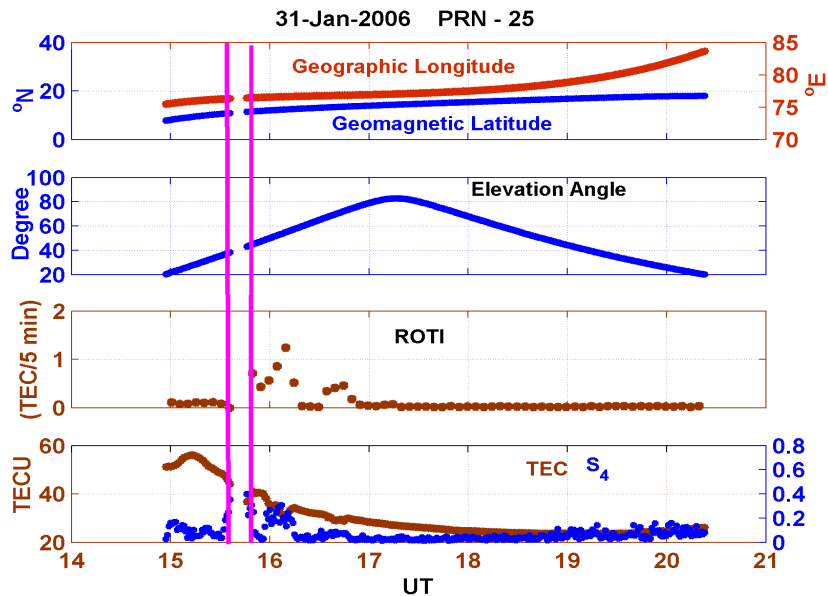


Fig. 5. Observations of depletion in TEC on 31 January 2005 for PRN-25. Same as Fig. 1.

Results obtained on 31 January 2006 for PRN 25 are shown in Fig. 5. The GMLAT and geographic longitude of the IPP for this satellite pass are plotted in the top panel of the figure. It can be seen clearly from the Fig. 5 that for the entire pass of the satellite, the range of GMLAT and longitude of the IPP is quite wide about 10° and 8° , respectively. The highest elevation attained by the satellite is about 80° . In Fig. 6 (left panel), the lock time of PRN 25 is shown and it is clear that the signal strength degrades during the passes of the irregularity.

A loss of lock of the signal is found due to sudden increase in scintillation activity. Sky plot in Fig. 6 (Right panel) shows the track of the PRN 25. In this case two consecutive depletions in TEC are found, wherein the values of TEC vary by about 12 TECU, observed between 15:30 UT and 16:15 UT. The satellite is nearly overhead at this hour, as revealed from the elevation ($\sim 40^\circ$). S4 index suddenly shoots up with the appearance of these depletions and is about 0.4. A nearly constant longitude of the IPP implies that these features are field aligned.

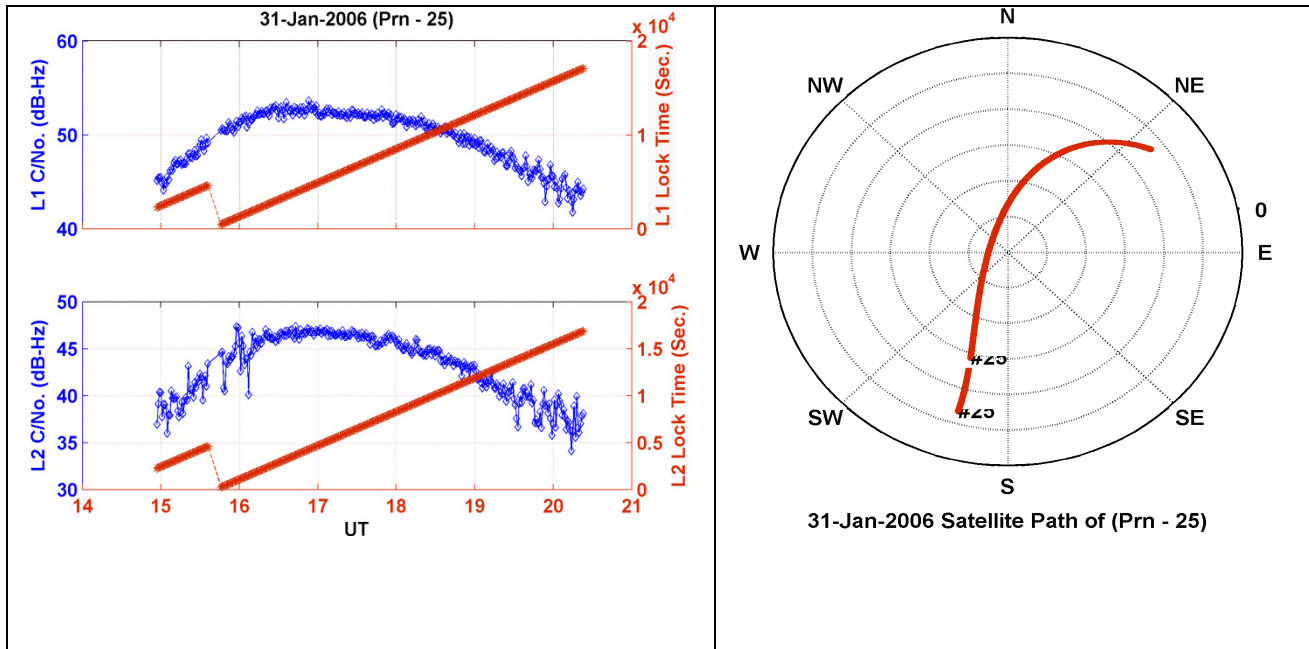


Fig. 6. Loss of lock of L1 and L2 signals and L1 and L2 carrier to noise ratio (Left panel) and Sky plot (Right panel) of PRN-25 for 31 January 2005.

B. Characteristics of Nighttime TEC Depletions

In the period from January 2005 to December 2006, nighttime depletion in TEC, occurrence time, time of dip occurrence are noted and subsequent analysis has been carried out. The distribution of nighttime TEC depletions during quiet and disturbed days in all months is presented in Fig. 7. Depletions in TEC are observed in both geomagnetic quiet and disturbed times. It is observed that the nighttime depletion in TEC at Bhopal occurs in all seasons. Fig. 8 shows the distribution of depletion for different seasons, Summer (May, June, July and August), Equinox (March, April, September and October) and Winter (November, December, January and February). It can be seen from Fig. 8 that occurrence of TEC depletions are maximum in winter

and minimum in summer months. The occurrence of TEC depletion maximizes during pre-midnight around 20:00 hrs IST in winter. During equinox it is delayed by about an hour around 21:00 hrs IST and during post-midnight around 01:00 hrs IST in summer. The occurrence of depletion is higher in pre-midnight hours than in post-midnight hours in all seasons. Number of occurrences is maximum in winter and least in summer. The occurrence of depletion during pre-midnight and post-midnight is shown in Fig. 9. It shows that maximum cases of depletion (26) were observed in pre-midnight during winter months and only three cases were found in post-midnight during the months of February and July.

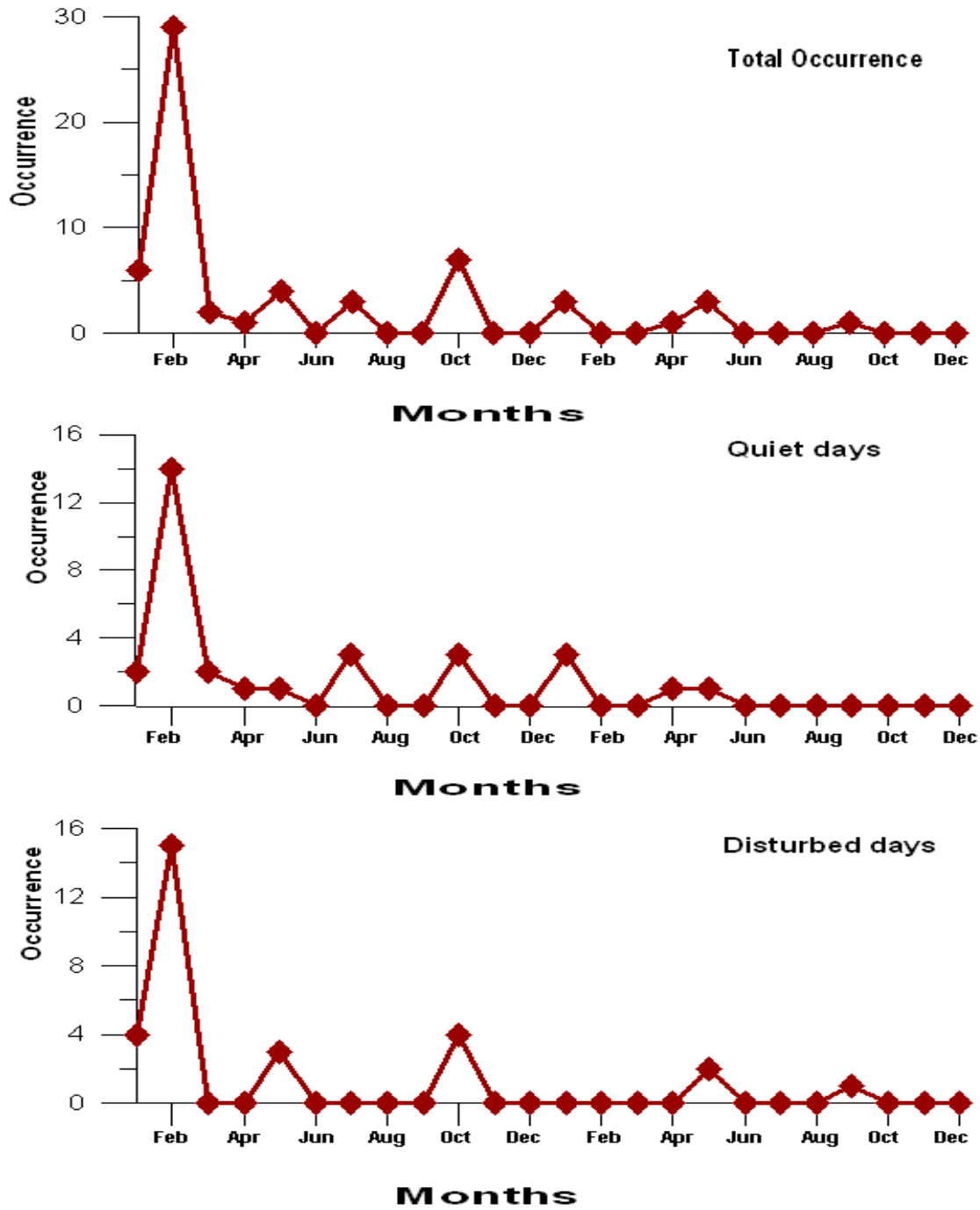


Fig. 7. Monthly occurrences of TEC depletions during geomagnetic quiet and disturbed conditions.

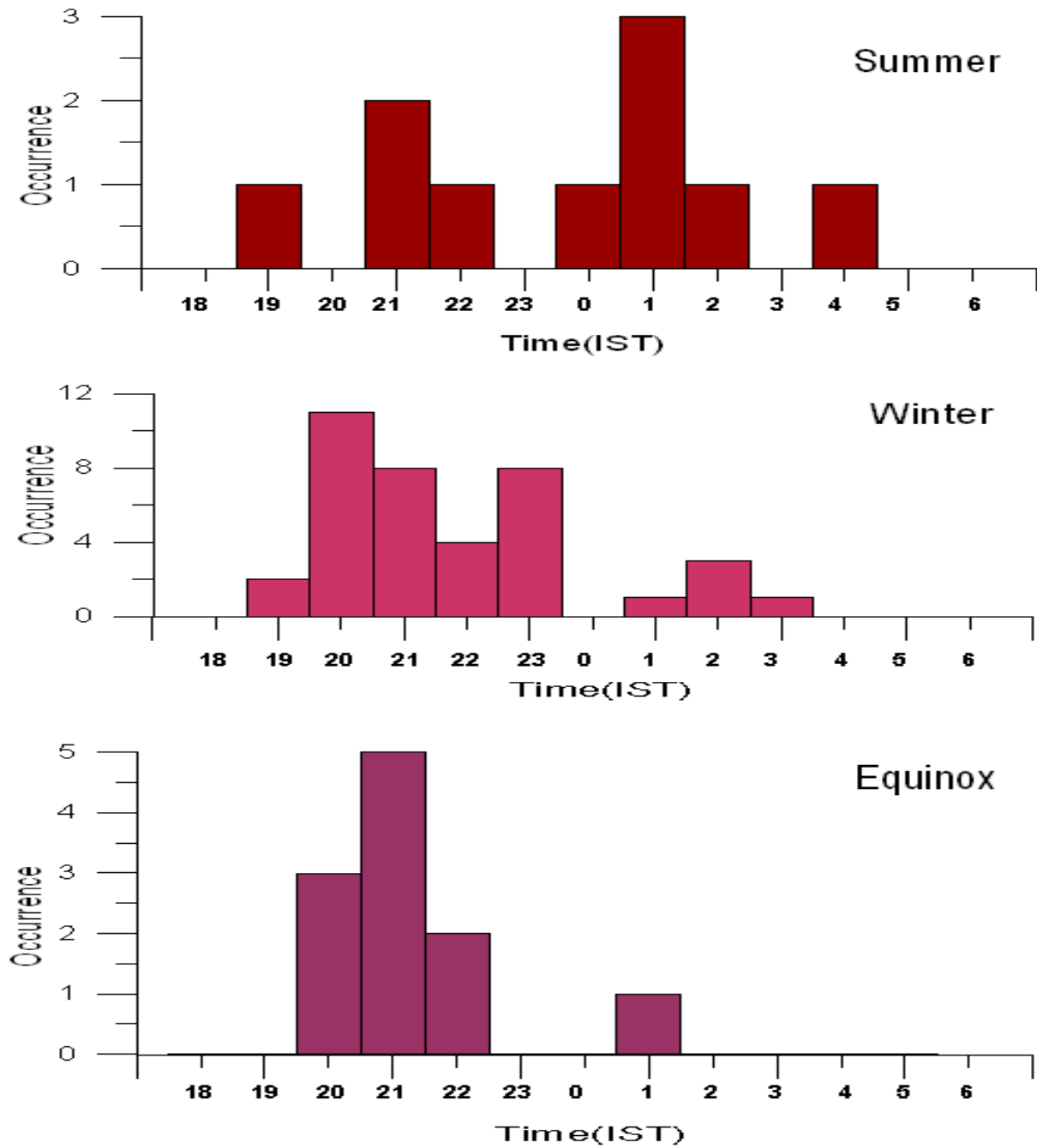


Fig. 8. Occurrence of the time of depletion in TEC for each season during 2005-06.

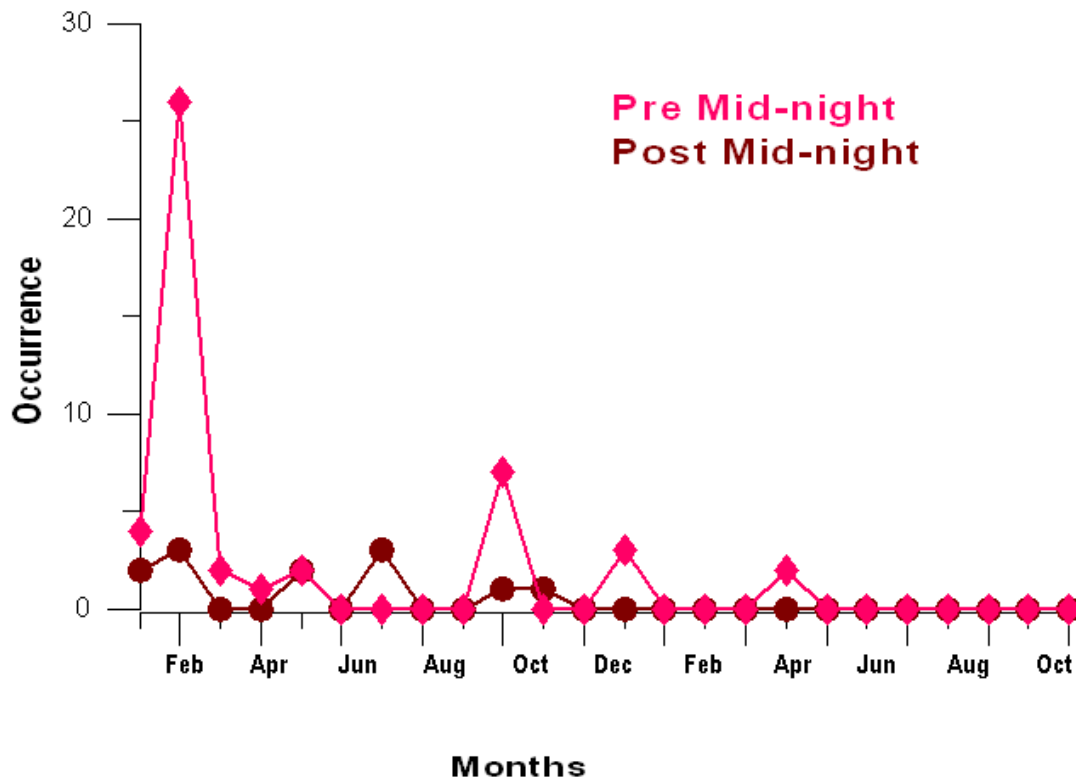


Fig. 9. Monthly variations of TEC depletions for Pre-midnight and Post-midnight hours.

IV. DISCUSSION

The occurrence of plasma bubbles in equatorial and EIA regions is reported by many workers [13-15, 21-22]. We have reported the first observations of nighttime TEC depletions at the equatorial anomaly crest region Bhopal using the GPS satellites. Generation of equatorial irregularities over the magnetic equator in the post sunset hours is intimately related to the variation of the height of the F-layer around sunset. The depletion that originates over the magnetic equator in the post sunset hours extends in both horizontal and vertical directions. The bubbles are up welled by electro dynamic EXB drift over the magnetic equator and they map down to the off-equatorial locations along magnetic field lines in the form of “bananas”. These bubbles may sometimes rise to greater heights, exceeding 1000 kms above the magnetic equator. The bubbles are generated at the bottom side of the equatorial F-region and move to the top side, will thus have signatures on the TEC. As the depletions are field-aligned, their uplift implies, uplifting of the entire flux tube. If the depletions rise to a sufficiently high altitude at the equator, the associated flux tube may connect to the equatorial anomaly zone latitudes. Since the F-region density heavily weights the TEC, any variation in the F-region plasma density should be reflected in the TEC. Sudden reductions in TEC, observed in the

nighttime low-latitude F-region have been identified with the plasma density depletion of the equatorial origin [26]. Consistent with this definition, the reduction in the TEC reported in figures 1 through 7 have been identified as manifestation of the plasma density depletion of equatorial origin. The depth of the depletions reported here is similar with the observations of other workers [27-29]. The presence of large depletion (plasma bubbles) is always accompanied with a very fast increase in the S4 index (S4). The increase in the S4 index is clearly seen at the time when the depletions in TEC are observed in all cases reported here. Occurrence and behavior of 137 MHz UHF amplitude scintillation and ionospheric TEC depletions recorded at Arequipa, Peru (16.4°S, 71.5°W; magnetic dip 9°S), during the solar maximum 1979-1980 was studied by [30]. They found that TEC depletions have typical duration of 10-15 min with amplitude less than 5 TECU. Mapping of the polarization electric fields associated with the depletions at the equator are responsible for the generation of the localized regions of plasma enhancements. According to this mechanism, the Rayleigh-Taylor plasma instability is excited within the limited latitudinal extent in the bottom side F region near the equator. The density depletion occurs near the equator. The polarization electric fields associated with these depletions lift them up at the equator.

While the depletions have a limited latitudinal extent, the polarization field maps to higher latitudes along the field lines. When the depletions rise to the top side F region at the equator, the flux tube associated with these depletions may be connecting the F peak in the anomaly zone latitudes. The mapped field in the anomaly zone thus moves the high-density plasma upward so that the density increments occur just above the flux tube.

Furthermore, they point out that the density increments are additionally reinforced if the background ionosphere moves downward. Mapping of the polarization fields associated with depletions would be efficient and effective, if the ionospheric region connected by the geomagnetic field lines has lower integrated pedersen conductivity than the region in which the fields are generated.

GPS has been used to locate and analyze plasma bubbles and irregularity regions at low latitudes [26-28]. Such type of plasma bubbles detected by GPS based systems have been reported near the equatorial anomaly latitude at Udiapur (24.6°N, 73.7°E.15.6°N GMLAT) for 5 and 28 October 2004 and 7 February 2005 by [25]. Detection of plasma bubbles using GPS based receiver over Pune and was done by [18]. The bubble normally drifts from west to east. As a bubble moves across a satellite link, ionization depletion and scintillation are usually encountered. The majority of the bubbles have duration less than 5 min with a maximum of 14 min. They also found associated bite-outs in TEC which moves from south-west to north-east nearly along a meridian during the time of depletion. Statistics of equatorial plasma bubble calculated from depletions in TEC in the local post-sunset hours near Pune, which is situated in between the magnetic equator and the northern crest of the equatorial anomaly in the Indian zone [18]. The statistics of nighttime TEC depletion have also been done here. The occurrence of depletion in TEC is found maximum in winter and minimum in summer. One more important finding of the present study is the occurrence of TEC depletions in localized time. We have reported maximum cases of depletions in pre-midnight hours in winter. This leads to the belief that the depletions in TEC are connected with the equatorial spread F.

V. CONCLUSIONS

Nighttime TEC depletions are studied using amplitude scintillation and TEC data recorded GPS ionospheric scintillation and TEC monitor at Bhopal. ROTI and losses of lock of the GPS signals have also been studied. The main outcomes of this work are as follows:

- The presence of large depletions (plasma bubbles) is always accompanied with very fast increase in the S4 index (S4).
- The ROTI value shows the strength of irregularity this is confirmed by the sudden TEC depletion and increase in the S4 value. Hence ROTI can alone be used as the irregularity index.
- The losses of lock occur during the encounter of the irregularity and the signal strength degrades during the passes of the irregularity.
- It is confirmed that north-south satellite trajectories show scintillations over a long period with transition from intense scintillation to no scintillations corresponding to crossing over the northern edge of the irregularity cloud.
- The occurrence of depletion in TEC is found maximum in winter and minimum in summer.
- Maximum cases of depletions are reported during pre-midnight hours in winter. This leads to the belief that the depletions in TEC are connected with the equatorial spread F.

REFERENCES

- [1]. Su Basu, S Basu, E. MacKenzie et al., (1988). Simultaneous density and electric field fluctuation spectra associated with velocity shears in the auroral oval. *Journal of Geophysical Research*, **93**, 115.
- [2]. M. C. Kelley, (1989). *The Earth's Ionosphere*. Elsevier, New York,.
- [3]. W. B. Hanson and S. Sanatani, (1973). Large Ni gradients below the equatorial spread-F peak. *Journal of Geophysical Research*, **78**, 1167-1173.
- [4]. R. F. Woodman, and C. La Hoz, (1976). Radar observations of F-region equatorial irregularities, *Journal of Geophysical Research*, **81**, 5447-5466.
- [5]. H.C. Yeh, S. Y. Su and R. A. Heelis, (2001). Storm time plasma irregularities in the pre-dawn hours observed by the low latitude ROCSAT-1 satellite at 600 km altitude, *Geophysics Research Letters*, **28**, 685-688.
- [6]. J. Aarons, (1993). The longitudinal morphology of equatorial F-layer irregularities relevant to their occurrence. *Space Science Review*, **63**, 209-263.
- [7]. D. J. Fang and M. S. Pontes, (1981). 4/6 GHz ionospheric scintillation measurements during the peak of sunspot cycle 21. *COMSAT Tech. Rev.*, **11**, 29-320.
- [8]. K. C. Yeh, H. Soicher, and C.H. Liu, (1979). Observations of equatorial ionospheric bubbles by the radio propagation method, *Journal of Geophysical Research*, **84**, 6589-6594.
- [9]. M. A. Abdu, I. S. Batista, J. H. A. Sobral, E. R. de Paula, and I. J. Kantor, (1985). Equatorial ionospheric plasma bubble irregularity occurrence and zonal velocities under quiet and disturbed conditions, from polarimeter observations. *Journal of Geophysical Research*, **90**, 9921-9928.

- [10]. T. Bandyopadhyay, A. Guha, A. Das Gupta, P. Banerjee, and A. Bose, (1997). Degradation of navigational accuracy with the Global Positioning System during periods of scintillation at equatorial latitudes., *Electrons. Lett.*, **33**(12), 1010-1011.
- [11]. P. M. Kintner, H. Kil, T. L. Bleach and E. R. de Paula, (2001). Fading timescales associated with GPS signals and potential consequences. *Radio Science*, **36**, 731-743.
- [12]. P. M. Kintner, B. M. Ledvina, E. R. de Paula and I. J. Kantor, (2004). Size, shape, orientation, speed and duration of GPS equatorial anomaly scintillations. *Radio Sci.*, **39**, RS2012, doi:10.1029/2003RS002878.
- [13]. A. Das Gupta, S. Ray, A. Paul, P. Banerjee and A. Bose, (2004). Errors in position- fixing by GPS in an environment of strong equatorial scintillations in the Indian zone, *Radio Science*, **39**, RS1S30, doi:10.1029/2002RS002822.
- [14]. F. S. Rodrigues, E. R. dePaula, M. A. Abdu, A. C. Jardim, K. N. Iyer, P. M. Kintner, and D. L. Hysell, (2004). Equatorial spread F irregularity characteristics over Sao Luis, Brazil, using VHF radar and GPS scintillation techniques. *Radio Sci.*, 2004, RS1S31, doi: 10.1029/2002RS002826.
- [15]. P.V.S Rama Rao, P.T. Jayachandran Sriram, B. V. Ramana Rao, D. S. V. V. D. Prasad and K. K. Bose, (1997). Characteristics of VHF radio wave scintillation over a solar cycle (1983-1993) at a low latitude station Walteir (17.7° N, 83.3° E). *Annales Geophysics (France)*, **15**, 729.
- [16]. A. Bhattacharya, K. M. Groves, S. Basu, H. Kuenzler, C. E. Valladares and R. Sheehan, (2003). L-band scintillation activity and space-time structure of low latitude UHF scintillations. *Radio Science(USA)*, **38**, 1004, doi: 10.1029/2002RS002711.
- [17]. P. V. S. Rama Rao, K. Niranjan, D. S. V. V. D. Prasad, S. Gopi Krishna, G Uma, (2006). On the validity of the ionospheric pierce point (IPP) altitude of 350 km in the Indian equatorial and low latitude sector. *Ann. Geophys.* **24**, 2159-2168.
- [18]. A. Das Gupta, A. Paul, S. Ray, A. Das and S. Ananthkrishnan, (2006). Equatorial bubbles as observed with GPS measurements over Pune, India. *Radio Science*, **41**, 1-11.
- [19]. R. Tiwari, S. Bhattacharya P.K. Purohit, and A.K. Gwal (2009). Effect of TEC Variation on GPS Precise Point at Low Latitude, *The Open Atmospheric Science Journal*, **3**, 1-12,
- [20]. Xifeng Liu, Yunbin Yuan, Bingfeng Tan and Min Li, (2016). Observational Analysis of Variation Characteristics of GPS-Based TEC Fluctuation over China *ISPRS Int. J. Geo-Inf.*, **5**, 237; doi:10.3390/ijgi5120237.
- [21]. A. K. Gwal, P. Bhawre, A. A. Mansoori, and P. A. Khan, (2013). Study of GPS Derived Total Electron Content and Scintillation Index Variations over Indian Arctic and Antarctic Stations *J. Sci. Res.* **5** (2), 255-264.
- [22]. Pi, X.; Mannucci, A.; Lindqwister, U.; Ho, C. (1997). Monitoring of global ionospheric irregularities using the worldwide GPS network. *Geophys. Res. Lett.*, **24**, 2283–2286.
- [23]. M. J. Birch, J. K. Hargreaves, and G. J. Bailey, (2002). On the use of an effective ionospheric height in electron content measurement by GPS reception. *Radio Science*, **37**, 1-19.
- [24]. C. E. Valladaras, and R. Sheehan, (2004). A latitudinal network of GPS receivers dedicated to studies of equatorial spread F. *Radio Science*, **39**.
- [25]. N. Dashora and R. Pandey, (2005). Observations in equatorial anomaly region of total electron content enhancements and depletions, *Annals Geophysics*, **23**, 2449-2456.
- [26]. A. Das Gupta, A. Paul and Das, (2007). Ionospheric total electron content (TEC) studies with GPS in the equatorial region. *Indian Journal of Radio and Space Physics*, **36**, 278-292.
- [27]. E. J. Weber, S. Basu, T. W. Bullet, C. E. Valladares, G. Bishop, K. Groves, H. Kuenzler, P. Ning, P. J. Sultan, R. E. Sheehan and J. Arya, (1996). Equatorial plasma depletion precursor signatures and onset observed at 11° south of the magnetic equator. *Journal of Geophysical Research*, **101**, 26829-26838.
- [28]. T. L Beach and P. M. Kintner, (1999). Simultaneous Global positioning system observations of equatorial scintillations and total electron content, *Journal of Geophysical Research*, **104**, 22553-22565.
- [29]. A. Bhattacharya, T. L. Beach and S. Basu, (2000). Nighttime equatorial ionosphere: GPS scintillations and differential carrier phase fluctuations. *Radio Sci.*, **35**, 209-224.
- [30]. A. Das Gupta, S. Basu, J. Aarons, A. Klobuchar and A. Bushby, (1983). VHF amplitude scintillations and associated electron content depletions as observed at Arequipa, Peru. *J. Atmos. Terr. Phys.*, **45**, 15-26.
- [31]. J. Aarons, M. Mendillo and R. Yantosca. (1996). GPS phase fluctuations in the equatorial region during the MISETA 1994 campaign, *Journal of Geophysical Research*, **101**, 26851.
- [32]. M.C. Kelley, D. Kotsikopoulos, T. Beach, D. Hysell and S. Musman, (1996). Simultaneous Global Positioning System and radar observations of equatorial spread F at Kwajalein. *Journal of Geophysical Research*, **101**, 2333.
- [33]. M. A. Cervera and R. M. Thomas, (2006). Latitudinal and temporal variation of equatorial ionospheric irregularities determined from GPS scintillation observations. *Annales Geophysics*, **24**, 3329-3341.